Journal of Computational and Applied Mathematics 420 (2023) 114834

Contents lists available at ScienceDirect

Journal of Computational and Applied Mathematics

journal homepage: www.elsevier.com/locate/cam

On C^2 cubic quasi-interpolating splines and their computation by subdivision via blossoming

D. Barrera [a,b,*], S. Eddargani [a,c], A. Lamnii [d]

[a] Department of Applied Mathematics, University of Granada, Campus de Fuentenueva s/n, 18071 Granada, Spain
[b] IMAG – Institute of Mathematics, Ventanilla 11, 18001 Granada, Spain
[c] Hassan First University of Settat, Faculté des Sciences et Techniques, Laboratoire MISI, Morocco
[d] Abdelmalek Essaadi University, LaSAD, ENS, 93030, Tetouan, Morocco

ARTICLE INFO

Article history:
Received 22 August 2021
Received in revised form 1 September 2022

Keywords:
Bernstein–Bézier representation
Cubic splines
Quasi-interpolation schemes
Subdivision rules

ABSTRACT

We discuss the construction of C^2 cubic spline quasi-interpolation schemes defined on a refined partition. These schemes are reduced in terms of degrees of freedom compared to those existing in the literature. Namely, we provide a rule for reducing them by imposing super-smoothing conditions while preserving full smoothness and cubic precision. In addition, we provide subdivision rules by means of blossoming. The derived rules are designed to express the B-spline coefficients associated with a finer partition from those associated with the former one.

1. Introduction

Spline functions are a mature and well-researched field in numerical analysis. The use of low degree polynomials is beneficial for curve fitting as they reduce the computational load and numerical instabilities that are typical of high degree polynomial interpolants. Cubic splines with continuity C^2 are very appealing because they couple the low degree with full smoothness which allows to efficiently address various problems.

Given a partition $X_n := \{x_i : a = x_0 < x_1 < \cdots < x_n = b\}$ of a bounded interval $I := [a, b]$, $C^2(I)$-continuous cubic splines can be constructed by decomposing each interval $I_i := [x_i, x_{i+1}]$, $0 \le i \le n-1$, into three micro-intervals after inserting two new knots [1,2]. More recently, the same idea has been used in [3,4] to address the problem of Hermite interpolation with this kind of cubic splines. In both papers, the constructed spline is expressed in each sub-interval I_i, in terms of its function and derivative values up to order two at the knots x_i and x_{i+1}. The spline is written as a linear combination of a set of basis functions. In [3], the considered basis is a classical Hermite basis, which means that the basis functions are not all non-negative, while the authors in [4] have provided a strategy to construct normalized B-spline-like bases, i.e., the basis functions form a partition of unity, are compactly supported and are all non-negative. These properties ensure both numerical stability and local control of the constructed spline. This approach is somewhat complicated, and may be seen as a special case of the approach used in this work.

The idea of inserting a split knot was first proposed in [5] which is considered as the univariate case of the Powell–Sabin (PS-)split [6,7]. It is widely used to approximate n-variate functions. In the case $n = 2$, this refinement into six micro-triangles was introduced in [8] to construct C^1-quadratic interpolating splines, leading to intensive research, in which the construction of B-spline-like function bases introduced in [9] should be highlighted. The cubic case was considered

* Corresponding author at: Department of Applied Mathematics, University of Granada, Campus de Fuentenueva s/n, 18071 Granada, Spain.
E-mail addresses: dbarrera@ugr.es (D. Barrera), seddargani@correo.ugr.es (S. Eddargani), a.lamnii@uae.ac.ma (A. Lamnii).

https://doi.org/10.1016/j.cam.2022.114834

in [10–14]. Quartic splines were also discussed in [15,16]. Spaces of quintic and sextic bivariate splines were analyzed in [17,18]. In [19,20], normalized bases for PS-splines of degree $3r-1$ and super-splines of arbitrary degree are given, respectively (see also [21,22]). In the case $n=3$, the construction of C^1-quadratic interpolants is given in [23]. Each tetrahedron in the tessellation is subdivided into 24 subtetrahedra in a specific way. This problem for a PS-refinement of a tessellation of s-simplices in $\mathbb{R}^s$ obtained by decomposing each of them into smaller simplices is addressed in [24].

Regarding the univariate case, quasi-interpolation operators expressed in Bernstein form are more suitable. In fact, the Bernstein basis of degree d relative to an interval I is the best basis in $\mathbb{P}_d$ restricted to I, according to the concept of optimal normalized totally positive basis [25,26]. Moreover inserting additional knots is often used to incorporate shape parameters in order to construct approximating splines that preserve convexity or monotonicity to given data [5]. Shape-preserving properties for the cubic spline space proposed in this work can be achieved by imposing conditions on the location of the new inserted knots to achieve simpler results than those available when using spaces without split points. Inserting new knots is used also in the bivariate case to preserve convexity [27].

We consider a space of C^1 continuous cubic splines on a refined partition with C^2 super-smoothness conditions at the set of split points recently introduced in [7], where a general framework for quasi-interpolation based on the cubic B-splines has been developed in [7]. The provided quasi-interpolating splines are C^1 continuous on I, and C^2 at the set of split points. The aim of this work is to provide a rule that will enforce the C^2 smoothness conditions at the set of knots, and later, on the whole domain. Motivated by [28], we develop a subdivision rule by means of blossom which provides the coefficients of the B-spline-like representation on the finer partition (twice-split) written as convex combinations of the B-spline-like coefficients on the former partition (simple-split). The convexity property is useful because it allows to get a stable computation and makes the subdivision geometrically intuitive. By means of the derived subdivision rule, we can provide a C^2 quasi-interpolating spline defined on the twice-refined partition like those splines in [3,4] but with a lower set of functional data.

In this work, we reduce the computational cost by considering a simple refinement of X_n obtained by introducing a single split point in each element of X_n. Then, a reduced space of C^2 cubic splines is defined from function values and first derivative values at the knots and from function values at the inserted split points. In summary, full smoothness is preserved and the number of degrees of freedom is reduced, so that the computational cost diminishes.

The paper is organized as follows. In Section 2, we provide some preliminaries on Bernstein–Bézier form and polar forms. Section 3 is devoted to introduce the space of C^1 cubic splines, to provide a representation of B-splines and to derive a rule that ensures the global C^2 smoothness on the whole domain. The theoretical results are confirmed by some numerical tests. In Section 4, subdivision rules are derived for the provided B-spline representation. Also some numerical tests are proposed to illustrate the convergence of the derived rules.

2. Preliminaries

In general, $S_d^r(X_n)$ will denote the space of C^r polynomial splines of degree d on X_n, i.e.

$$S_d^r(X_n) := \left\{ s \in C^r(I) : \ s_{|I_i} \in \mathbb{P}_d, \ i=0,\dots,n-1 \right\},$$

where $\mathbb{P}_d$ stands for the space of polynomials of degree less than or equal to d.

The restriction of each element s of $S_d^r(X_n)$ to an interval I_i is a polynomial. Then, it can be represented in the Bernstein basis relative to I_i by using the barycentric coordinates $(1-t, t)$ with respect to I_i, i.e. $x=(1-t)\,x_i+tx_{i+1}$ holds. Using the notations $|\boldsymbol{\alpha}| := \alpha_1+\alpha_2$ for the length of a multi-index $\boldsymbol{\alpha} := (\alpha_1,\alpha_2)$ with non-negative integer entries and $\boldsymbol{\alpha}! := \alpha_1!\alpha_2!$, the Bernstein polynomials $\mathfrak{B}_{\boldsymbol{\alpha},i}^d$ of degree d relative to I_i is given by

$$\mathfrak{B}_{\boldsymbol{\alpha},i}^d(x) = \frac{d!}{\boldsymbol{\alpha}!}(1-t)^{\alpha_1}\ t^{\alpha_2}, \ \ |\boldsymbol{\alpha}| = d. \tag{1}$$

Each polynomial $\mathfrak{B}_{\boldsymbol{\alpha},i}^d$ is non-negative whenever $0 \le t \le 1$, i.e. when $x \in I_i$.

Each polynomial $p \in \mathbb{P}_d$ can be expressed on I_i as a convex combination of polynomials $\mathfrak{B}_{\boldsymbol{\alpha},i}^d$, so that there exist coefficients $b_{\boldsymbol{\alpha},i}$, $|\boldsymbol{\alpha}| = d$, such that

$$p = \sum_{|\boldsymbol{\alpha}|=d} b_{\boldsymbol{\alpha},i}\,\mathfrak{B}_{\boldsymbol{\alpha},i}^d.$$

It is the Bernstein–Bézier (BB-) representation of p and its coefficients are said to be the Bézier (B-) ordinates or Bernstein–Bézier (BB-) coefficients of p relative to I_i. They are linked to the domain points $\Lambda_{\boldsymbol{\alpha},i} := \frac{\alpha_1}{d}x_i + \frac{\alpha_2}{d}x_{i+1}$. By linking each B-ordinate $b_{\boldsymbol{\alpha},i}$ with the domain point $\Lambda_{\boldsymbol{\alpha},i}$, the BB-representation can be displayed schematically as shown in Fig. 1 for the case of cubic polynomials. The piecewise linear interpolant of the control points $c_{\alpha,i} := \left(\Lambda_{\boldsymbol{\alpha},i}, b_{\boldsymbol{\alpha},i}\right)$ is said to be the control net. It is tangent to the polynomial curve at the two knots x_i and x_{i+1}.

The B-ordinates $b_{\boldsymbol{\alpha},i}$ can be explicitly determined from the polar form or blossom $\mathcal{B}[p]$ [29], i.e. the unique symmetric multi-affine polynomial $\mathcal{B}[p] : \mathbb{R}^d \to \mathbb{R}$ fulfilling the diagonal property $\mathcal{B}[p](x[d]) = p(x)$, where $x[d]$ means that the point x is repeated d times as an argument of the polar form, omitting the term $[d]$ when $d=1$. More specifically, it holds

$$b_{\boldsymbol{\alpha},i} = \mathcal{B}[p](x_i[\alpha_1],\ x_{i+1}[\alpha_2]).$$

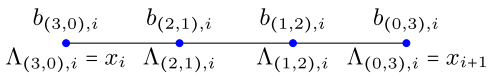

Fig. 1. Schematic representation of the domain points and B-ordinates of a cubic polynomial.

Another very useful practical utility of polar forms is the computation of the B-ordinates of the restriction of a polynomial p to a sub-interval of I from the ones of p relative to I. For a sub-interval $\tilde{I} = [c_1, c_2]$ of I, with c_1 and c_2 having barycentric coordinates $\sigma^i = \left(\sigma_1^i, \sigma_2^i\right)$, $i = 1, 2$, with respect to I, then the B-ordinates $\tilde{b}_{\boldsymbol{\alpha}}$ of p on $\tilde{I}$ can be determined in the following form:

$$\tilde{b}_{\boldsymbol{\alpha},i} = \mathcal{B}[p]\left(\sigma^1[\alpha_1],\ \sigma^2[\alpha_2]\right). \tag{2}$$

Also the De Casteljau's algorithm is used to calculate the blossom in a stable way. Only convex combinations are produced:

$$\mathcal{B}[p]\left(\tau^1, \ldots, \tau^d\right) = b_{(0,0)}^{[d]},$$

where

$$b_{\boldsymbol{\alpha}}^{[0]} = b_{\boldsymbol{\alpha},i},\ \text{for } |\boldsymbol{\alpha}| = d,$$
$$b_{\boldsymbol{\alpha}}^{[r]} = \tau_1^r b_{\boldsymbol{\alpha}+e_1}^{[r-1]} + \tau_2^r b_{\boldsymbol{\alpha}+e_2}^{[r-1]},\ \text{for } |\boldsymbol{\alpha}| = d-r,\ \text{and } r = 1, \ldots, d,$$

with $e_1 := (1, 0)$ and $e_2 := (0, 1)$. For details, see [7].

3. Reduced C^2 cubic splines space

In what follows, we start from a space of C^1 cubic splines and then a rule to achieve C^2 regularity on an arbitrary partition is given.

3.1. C^1 Cubic splines

Let $\widetilde{X}_n$ be the refinement of X_n obtained by inserting in every I_i a split point ξ_i. We focus on the subspace $S_3^{1,2}\left(\widetilde{X}_n\right)$ of $S_3^1\left(\widetilde{X}_n\right)$ resulting when C^2 smoothness at the inserted knots [7] is required, i.e.

$$S_3^{1,2}\left(\widetilde{X}_n\right) := \left\{s \in S_3^1\left(\widetilde{X}_n\right) : s \in C^2(\xi)\right\},$$

where $\boldsymbol{\xi} := \{\xi_i\}_{i=1}^{n-1}$ is the set of the inserted split points. Hereafter, the elements of X_n will be called knots, while we will refer to the inserted points ξ_i as inner split points.

A spline $s \in S_3^{1,2}\left(\widetilde{X}_n\right)$ can be uniquely characterized by specifying two particular values for each knot of X_n, and one value for each interval induced by X_n.

Theorem 1. *Given values f_i^0, and f_i^1, $0 \le i \le n$, and g_i, $0 \le i \le n-1$, there exists a unique spline $s \in S_3^{1,2}\left(\widetilde{X}_n\right)$ such that*

$$s(x_i) = f_i^0, \quad s'(x_i) = f_i^1 \tag{3}$$

for every knot x_i of X_n and

$$s(\xi_i) = g_i \tag{4}$$

for every interval I_i.

Proof. It suffices to show how the B-ordinates of the solution $s \in S_3^{1,2}\left(\widetilde{X}_n\right)$ of this non standard interpolation problem are obtained for each macro-interval I_i.

On each of the two micro-intervals $J_{i,1} := [x_i, \xi_i]$ and $J_{i,2} := [\xi_i, x_{i+1}]$ the spline s is a polynomial of degree 3, which can be represented from its B-ordinates. They are shown in Fig. 2. Any reference to I_i is omitted.

The B-ordinates d_0, d_1, d_2 and d_3 indicated by (•) are provided by the conditions in (3) on the values of the spline and its first derivative at knots x_i and x_{i+1}.

The interpolation condition at ξ_i given in (4) allows to compute the B-ordinate d_4 indicated by (▲). The remaining B-ordinates d_5 and d_6 indicated by (○), are computed from C^2 smoothness at ξ_i. More precisely, let p be a quadratic polynomial defined on the segment $[\frac{2x_i+\xi_i}{3}, \frac{\xi_i+2x_{i+1}}{3}]$. The B-ordinates of p are $b_{(2,0)} = d_1$, $b_{(1,1)} = \frac{1}{2\tau_{i,1}\tau_{i,2}}\left(d_4 - \tau_{i,1}^2 d_1 - \tau_{i,2}^2 d_2\right)$ and $b_{(0,2)} = d_2$, where, $\tau_{i,1}$ and $\tau_{i,2} = 1 - \tau_{i,1}$ are the barycentric coordinates of ξ_i with respect to I_i. After subdivision and by using (2), it follows that

$$d_5 = \mathcal{B}[p]\left((1,0),(\tau_{i,1},\tau_{i,2})\right) \text{ and } d_6 = \mathcal{B}[p]\left((\tau_{i,1},\tau_{i,2}),(0,1)\right).$$

It holds $d_5 = \tau_{i,1}d_1 + \tau_{i,2}b_{(1,1)}$ and $d_6 = \tau_{i,1}b_{(1,1)} + \tau_{i,2}d_2$, which concludes the proof. □

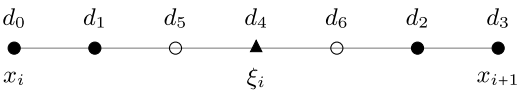

Fig. 2. A schematic representation of the B-ordinates involved in Theorem 1.

Having proved the unisolvency of the interpolation problem, we consider how to represent its unique solution. To do so, we construct B-spline-like functions (B-splines for short) $\mathcal{D}^{\mathrm{kn}}_{i,(\ell,m)}$, $\ell, m \in \mathbb{N}$, $\ell + m = 1$, and $\mathcal{D}^{\mathrm{sp}}_{k}$ in order to express any spline $s \in S_3^{1,2}\left(\widetilde{X}_n\right)$ in the form

$$s = \sum_{i=0}^{n} \sum_{\ell+m=1} c^{\mathrm{kn}}_{i,(\ell,m)}\, \mathcal{D}^{\mathrm{kn}}_{i,(\ell,m)} + \sum_{k=0}^{n-1} c^{\mathrm{sp}}_{k}\, \mathcal{D}^{\mathrm{sp}}_{k}. \tag{5}$$

The superscripts "kn" (knot) and "sp" (split) are used to distinguish between B-splines with respect to a knot and a split point, respectively. A B-spline with respect to a split point can also be designated as a B-spline with respect to the interval in which the split point is located.

We now show how to construct suitable B-splines $\mathcal{D}^{\mathrm{kn}}_{i,(\ell,m)}$ and $\mathcal{D}^{\mathrm{sp}}_{k}$ for the knot x_i and the interval I_k, respectively. The construction used herein is entirely based on the choice of a single interval $W_i := [W_{i,1}, W_{i,2}]$ for every knot x_i in X_n (see [7]). For each interior knot x_i, define

$$W_{i,1} := \frac{2}{3}x_{i-1} + \frac{1}{3}x_i \quad \text{and} \quad W_{i,2} := \frac{2}{3}x_{i+1} + \frac{1}{3}x_i. \tag{6}$$

One possibility to choose W_i is to consider the segment of minimal length that ensures the non-negativity of B-splines $\mathcal{D}^{\mathrm{kn}}_{i,(\ell,m)}$ [7]. In general, the choice depends on the problem being addressed, for more details see [30]. Equipped with W_i, we introduce four parameters corresponding to the knot x_i. Let $\left(\alpha_{i,(1,0)},\ \alpha_{i,(0,1)}\right)$ be the barycentric coordinates of x_i w.r.t. W_i. This is the unique pair satisfying

$$\alpha_{i,(1,0)}W_{i,1} + \alpha_{i,(0,1)}W_{i,2} = x_i, \quad \alpha_{i,(1,0)} + \alpha_{i,(0,1)} = 1.$$

Furthermore, let $\left(\beta_{i,(1,0)},\ \beta_{i,(0,1)}\right)$ be the directional barycentric coordinates of the vector $\overrightarrow{x}$ w.r.t. W_i. This is the unique pair such that

$$\beta_{i,(1,0)}W_{i,1} + \beta_{i,(0,1)}W_{i,2} = 1, \quad \beta_{i,(1,0)} + \beta_{i,(0,1)} = 0.$$

We define the B-spline basis for $S_3^{1,2}\left(\widetilde{X}_n\right)$ in terms of conditions (3) and (4) provided in Theorem 1. The definition of the B-splines $\mathcal{D}^{\mathrm{kn}}_{i,(\ell,m)}$, $\ell + m = 1$, corresponding to the knot x_i is based on $\alpha_{i,(\ell,m)}$ and $\beta_{i,(\ell,m)}$: at x_i we set

$$\mathcal{D}^{\mathrm{kn}}_{i,(\ell,m)}(x_i) = \alpha_{i,(\ell,m)}, \quad \left(\mathcal{D}^{\mathrm{kn}}_{i,(\ell,m)}\right)'(x_i) = \beta_{i,(\ell,m)},$$

and

$$\mathcal{D}^{\mathrm{kn}}_{i,(\ell,m)}\left(x_j\right) = 0, \quad \left(\mathcal{D}^{\mathrm{kn}}_{i,(\ell,m)}\right)'\left(x_j\right) = 0$$

at any knot x_j of X_n different from x_i. Moreover, if $\tau_{i,1}$ and $\tau_{i,2}$ are convex weights such that $\xi_i = \tau_{i,1}x_i + \tau_{i,2}x_{i+1}$, then we set the values in condition (4) to zero except

$$\mathcal{B}\left[\mathcal{D}^{\mathrm{kn}}_{i,(\ell,m)}\right](\xi_i[3]) = \tau_{i,1}^2\left(\alpha_{i,(\ell,m)} + \beta_{i,(\ell,m)}\frac{\xi_i - x_i}{3}\right)$$

and

$$\mathcal{B}\left[\mathcal{D}^{\mathrm{kn}}_{i,(\ell,m)}\right](\xi_{i-1}[3]) = \tau_{i-1,2}^2\left(\alpha_{i,(\ell,m)} + \beta_{i,(\ell,m)}\frac{\xi_{i-1} - x_i}{3}\right).$$

Similarly, we define the B-spline $\mathcal{D}^{\mathrm{sp}}_{k}$ corresponding to I_k by the setting all values in (3) and (4) to zero, except the following one:

$$\mathcal{B}\left[\mathcal{D}^{\mathrm{sp}}_{k}\right](\xi_k[3]) = 2\tau_{k,1}\tau_{k,2}.$$

Fig. 3 shows the typical plots of B-splines $\mathcal{D}^{\mathrm{kn}}_{i,(1,0)}$ and $\mathcal{D}^{\mathrm{kn}}_{i,(0,1)}$ associated with the interior knot x_i, as well as the B-spline $\mathcal{D}^{\mathrm{sp}}_{k}$ relative to the split point ξ_k.

Once constructed the B-splines as solutions of the corresponding interpolation problems, one needs to give the explicit expressions of coefficients $c^{\mathrm{kn}}_{i,(\ell,m)}$ and c^{sp}_{k} in the BB-representation (5) of $s \in S_3^{1,2}\left(\widetilde{X}_n\right)$. This is achieved by means of polar forms of restrictions of s to specific intervals of X_n. To be precise, for any interval J_i of X_n with an end-point at x_i, it holds

$$c^{\mathrm{kn}}_{i,(\ell,m)} = \mathcal{B}\left[s_{|J_i}\right](x_i[2],\ x_{i-1}[\ell],\ x_{i+1}[m]). \tag{7}$$

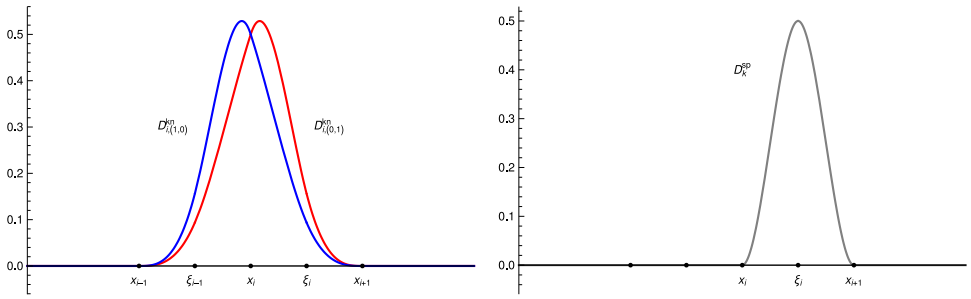

Fig. 3. B-splines with respect to the knot x_i (left), and the split point ξ_k (right).

Note that the above blossom value can be evaluated in terms of s and its first derivative at the knot x_i, namely

$$\mathcal{B}\left[s_{|J_i}\right](x_i[2],\, x_{i-1}) = s(x_i) + \frac{2}{3}s'(x_i)(x_{i-1} - x_i)$$

and

$$\mathcal{B}\left[s_{|J_i}\right](x_i[2],\, x_{i+1}) = s(x_i) + \frac{2}{3}s'(x_i)(x_{i+1} - x_i).$$

This confirms that the value of $c^{\mathrm{kn}}_{i,(\ell,m)}$ is independent of the choice of J_i. Regarding the coefficient c^{sp}_k corresponding to I_k, it is satisfied that

$$c^{\mathrm{sp}}_k = \mathcal{B}\left[s_{|J_k}\right](x_k,\, x_{k+1},\, \xi_k). \tag{8}$$

To understand the super-smoothness condition C^2 at the knots in X_n for C^1 cubic splines that we will explore later, we now review the Bernstein–Bézier representation of s restricted to an interval induced by $\widetilde{X}_n$. Let $J_{i,1} = [x_i,\, \xi_i]$ be the left sub-interval of I_i. The blossom value providing the B-ordinate of $s_{|J_{i,1}}$ corresponding to the knot x_i is given by

$$\mathcal{B}\left[s_{|J_{i,1}}\right](x_i[3]) = \sum_{\ell+m=1} \alpha_{i,(\ell,m)}\, c^{\mathrm{kn}}_{i,(\ell,m)}.$$

The B-ordinate corresponds to the domain point $\frac{2}{3}x_i + \frac{1}{3}\xi_i$ and is equal to

$$\mathcal{B}\left[s_{|J_{i,1}}\right](x_i[2],\, \xi_i) = \sum_{\ell+m=1} \left(\alpha_{i,(\ell,m)} + \beta_{i,(\ell,m)}\frac{\xi_i - x_i}{3}\right) c^{\mathrm{kn}}_{i,(\ell,m)}. \tag{9}$$

Note that the weights in the sum (9) are the barycentric coordinates of the $\frac{2}{3}x_i + \frac{1}{3}\xi_i$ w.r.t. W_i.

Furthermore, the B-ordinate corresponding to the split point ξ_i is

$$\mathcal{B}\left[s_{|J_{i,1}}\right](\xi_i[3]) = \tau^2_{i,1}\mathcal{B}\left[s_{|J_{i,1}}\right](x_i,\, \xi_i[2]) + \tau^2_{i,2}\mathcal{B}\left[s_{|J_{i,2}}\right](x_{i+1},\, \xi_i[2]) + 2\tau_{i,1}\tau_{i,2}\, c^{\mathrm{sp}}_k,$$

where $J_{i,2} = [\xi_i,\, x_{i+1}]$.

The B-ordinate corresponding to the domain point $\frac{1}{3}x_i + \frac{2}{3}\xi_i$ is a convex combination of certain B-ordinates associated with the domain points $\frac{2}{3}x_i + \frac{1}{3}\xi_i$ and ξ_i. Indeed, it is given by

$$\mathcal{B}\left[s_{|J_{i,1}}\right](x_i,\, \xi_i[2]) = \tau_{i,1}\mathcal{B}\left[s_{|J_{i,1}}\right](x_i[2],\, \xi_i) + \tau_{i,2}c^{\mathrm{sp}}_i.$$

In summary,

Remark 1. Boundary B-spline-like bases for $S^{1,2}_3\left(\widetilde{X}_n\right)$ are constructed according to the same procedure outlined for interior points. The B-spline-like w.r.t. vertex $a = x_0$ (resp. $b = x_n$) is constructed with a particular choice of the interval W_0 (resp. W_n). Namely,

$$W_{0,1} := x_0 \quad \text{and} \quad W_{n,2} := x_n.$$

Remark 2. Here, we show the relationship between the B-splines considered in this paper and the classical Hermite basis. Let φ_i and ψ_i be the unique functions in $S^{1,2}_3\left(\widetilde{X}_n\right)$ satisfying the interpolation conditions

$$\varphi_i(x_j) = \delta_{ij}, \quad \varphi_i'(x_j) = 0, \quad j = 0, \ldots, n,$$
$$\psi_i(x_j) = 0, \quad \psi_i'(x_j) = \delta_{ij}, \quad j = 0, \ldots, n,$$

where δ stands for Kronecker's delta.

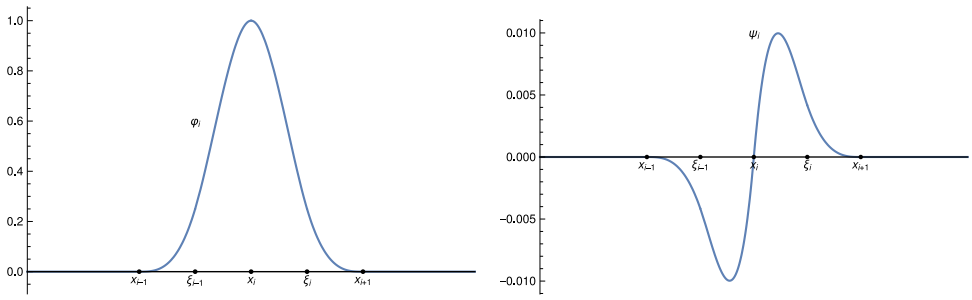

Fig. 4. The classical Hermite basis functions φ_i and ψ_i of the space $S_3^{1,2}\left(\widetilde{X}_n\right)$.

The B-splines $\mathcal{D}^{\mathrm{kn}}_{i,(\ell,m)}$, $\ell+m=1$, are convex combinations of the classical Hermite basis functions (see Fig. 4). Namely,

$$\mathcal{D}^{\mathrm{kn}}_{i,(\ell,m)} = \alpha_{i,(\ell,m)}\varphi_i + \beta_{i,(\ell,m)}\psi_i.$$

It can be proved that the B-splines considered here are convex combination of the B-splines lying in the space of cubic splines having double knots at knots x_i and simple knots at inner points ξ_i. For more details, see [31, ch. 9].

3.2. Rule to achieve C^2 smoothness at the set of knots

Consider a linear operator $\mathcal{Q}$ of the form

$$\mathcal{Q}f := \sum_{i=0}^{n}\sum_{\ell+m=1}\psi^{\mathrm{kn}}_{i,(\ell,m)}(f)\,\mathcal{D}^{\mathrm{kn}}_{i,(\ell,m)} + \sum_{k=0}^{n-1}\psi^{\mathrm{sp}}_{k}(f)\,\mathcal{D}^{\mathrm{sp}}_{k}, \tag{10}$$

which associates with a given function f a spline in $S_3^{1,2}\left(\widetilde{X}_n\right)$. It is based on the choice of linear functionals $\psi^{\mathrm{kn}}_{i,(\ell,m)}$ and ψ^{sp}_{k} corresponding to knots and intervals, respectively. Motivated by (7) and (8), we consider the linear functionals $\psi^{\mathrm{kn}}_{i,(\ell,m)}$ and ψ^{sp}_{k} given by

$$\begin{aligned}\psi^{\mathrm{kn}}_{i,(\ell,m)}(f) &= \mathcal{B}\left[\mathcal{I}^{\mathrm{kn}}_{i,(\ell,m)}f\right](x_i[2],\, x_{i-1}[\ell],\, x_{i+1}[m]),\\ \psi^{\mathrm{sp}}_{k}(f) &= \mathcal{B}\left[\mathcal{I}^{\mathrm{sp}}_{k}f\right](x_k,\, x_{k+1},\, \xi_k),\end{aligned} \tag{11}$$

for some linear operators $\mathcal{I}^{\mathrm{kn}}_{i,(\ell,m)}$ and $\mathcal{I}^{\mathrm{sp}}_{k}$ that map a function f to cubic polynomials $\mathcal{I}^{\mathrm{kn}}_{i,(\ell,m)}f$ and $\mathcal{I}^{\mathrm{sp}}_{k}f$. To guarantee the locality property of the quasi-interpolant, we assume that the data-sites of the scattered data used to construct $\psi^{\mathrm{kn}}_{i,(\ell,m)}$ (resp. ψ^{sp}_{k}) belong to the support of $\mathcal{D}^{\mathrm{kn}}_{i,(\ell,m)}$ (resp. $\mathcal{D}^{\mathrm{sp}}_{k}$) and allow us to construct a local linear polynomial operator $\mathcal{I}^{\mathrm{kn}}_{i,(\ell,m)}$ (resp. $\mathcal{I}^{\mathrm{sp}}_{k}$) reproducing the space of cubic polynomials [2,7,17,18,32], i.e., $\mathcal{I}^{\mathrm{kn}}_{i,(\ell,m)}f = f$ and $\mathcal{I}^{\mathrm{sp}}_{k}f = f$ for all $f\in\mathbb{P}_3$. One can choose the operators $\mathcal{I}^{\mathrm{kn}}_{i,(\ell,m)}$ and $\mathcal{I}^{\mathrm{sp}}_{k}$ as Lagrange or Hermite interpolation operators.

In what follows, we provide an approach that enables us to get C^2 smoothness at the knots in X_n. We start by observing from (7), (10) and (11) that

$$\begin{aligned}\mathcal{B}\left[\mathcal{I}^{\mathrm{kn}}_{i,(\ell,m)}f_{|J_{i,1}}\right](x_i[2],\, x_{i-1}[\ell],\, x_{i+1}[m]) &= \mathcal{B}\left[\mathcal{Q}f_{|J_{i,1}}\right](x_i[2],\, x_{i-1}[\ell],\, x_{i+1}[m]),\\ \mathcal{B}\left[\mathcal{I}^{\mathrm{sp}}_{k}f_{|J_{k,1}}\right](x_k,\, x_{k+1},\, \xi_k) &= \mathcal{B}\left[\mathcal{Q}f_{|J_{k,1}}\right](x_k,\, x_{k+1},\, \xi_k).\end{aligned}$$

As the following result shows, C^2 smoothness can be achieved by specifying a cubic polynomial that *connect* the local operators acting in the closest neighborhood of the knot.

Theorem 2. *Let $\mathcal{Q}f$ be defined by (10), and let x_i be a knot of X_n. Assume that there exists a polynomial $p\in\mathbb{P}_3$ such that the following requirements are met:*

1. *The operator $\mathcal{I}^{kn}_{i,(\ell,m)}$, $\ell+m=1$, corresponding to x_i satisfies*

$$\mathcal{I}^{kn}_{i,(\ell,m)}f(x_i) = p(x_i), \quad \left(\mathcal{I}^{kn}_{i,(\ell,m)}f\right)'(x_i) = p'(x_i). \tag{12}$$

2. *The operators $\mathcal{I}^{sp}_{i-1}$ and $\mathcal{I}^{sp}_{i}$ corresponding to the intervals I_{i-1} and I_i with an end-point at x_{i-1} and x_i, respectively, satisfy the conditions*

$$\mathcal{I}^{sp}_{i-1}f(\xi_{i-1}) = p(\xi_{i-1}), \tag{13}$$

$$\mathcal{I}^{sp}_{i}f(\xi_i) = p(\xi_i). \tag{14}$$

Then, $\mathcal{Q}f$ is C^2-continuous at x_i.

Proof. We need to prove that $(\mathcal{Q}f)''(x_i) = p''(x_i)$. Recall that,

$$\begin{aligned} D^2_{\xi_i - x_i}\, \mathcal{Q}f_{|J_{i,1}}(x_i) &= 6\,\mathcal{B}\left[\mathcal{Q}f_{|J_{i,1}}\right](x_i, (\xi_i - x_i)[2]) \\ &= 6\left(-2\mathcal{B}\left[\mathcal{Q}f_{|J_{i,1}}\right](x_i[2], \xi_i) + \mathcal{B}\left[\mathcal{Q}f_{|J_{i,1}}\right](x_i, \xi_i[2]) + \mathcal{B}\left[\mathcal{Q}f_{|J_{i,1}}\right](x_i[3])\right). \end{aligned}$$

and,

$$\begin{aligned} D^2_{x_i - \xi_{i-1}}\, \mathcal{Q}f_{|J_{i-1,2}}(x_i) &= 6\,\mathcal{B}\left[\mathcal{Q}f_{|J_{i-1,2}}\right](x_i, (x_i - \xi_{i-1})[2]) \\ &= 6\left(-2\mathcal{B}\left[\mathcal{Q}f_{|J_{i-1,2}}\right](x_i[2], \xi_{i-1}) + \mathcal{B}\left[\mathcal{Q}f_{|J_{i-1,2}}\right](x_i, \xi_{i-1}[2]) + \mathcal{B}\left[\mathcal{Q}f_{|J_{i-1,2}}\right](x_i[3])\right). \end{aligned}$$

More precisely, we need to prove that

$$D^2_{\xi_i - x_i}\, \mathcal{Q}f_{|J_{i,1}}(x_i) = 6\left(-2\mathcal{B}[p](x_i[2], \xi_i) + \mathcal{B}[p](x_i, \xi_i[2]) + \mathcal{B}[p](x_i[3])\right),$$

and,

$$D^2_{x_i - \xi_{i-1}}\, \mathcal{Q}f_{|J_{i-1,2}}(x_i) = 6\left(-2\mathcal{B}[p](x_i[2], \xi_{i-1}) + \mathcal{B}[p](x_i, \xi_{i-1}[2]) + \mathcal{B}[p](x_i[3])\right),$$

where the blossom values of p are all independent of $J_{i,1}$ and $J_{i-1,2}$, respectively. To this end, we consider the blossom values

$$\mathcal{B}\left[\mathcal{Q}f_{|J_{i,1}}\right](x_i[2], \xi_i), \quad \mathcal{B}\left[\mathcal{Q}f_{|J_{i,1}}\right](x_i, \xi_i[2]), \quad \mathcal{B}\left[\mathcal{Q}f_{|J_{i-1,2}}\right](x_i[2], \xi_{i-1}) \text{ and } \mathcal{B}\left[\mathcal{Q}f_{|J_{i-1,2}}\right](x_i, \xi_{i-1}[2])$$

that will help us to express the second order derivatives of $\mathcal{Q}f_{|J_{i,1}}$ and $\mathcal{Q}f_{|J_{i-1,2}}$ at the knot x_i.

The blossom value $\mathcal{B}\left[\mathcal{Q}f_{|J_{i,1}}\right](x_i[2], \xi_i)$ is the B-ordinate of $\mathcal{Q}f_{|J_{i,1}}$ on $J_{i,1}$ corresponding to the domain point $\frac{2}{3}x_i + \frac{1}{3}\xi_i$ (9), i.e.

$$\mathcal{B}\left[\mathcal{Q}f_{|J_{i,1}}\right](x_i[2],\ \xi_i) = \sum_{\ell+m=1}\left(\alpha_{i,(\ell,m)} + \beta_{i,(\ell,m)}\frac{\xi_i - x_i}{3}\right)\mathcal{B}\left[\mathcal{I}^{\mathrm{kn}}_{i,(\ell,m)}f\right](x_i[2],\ x_{i-1}[\ell],\ x_{i+1}[m]).$$

The weights $\alpha_{i,(\ell,m)} + \beta_{i,(\ell,m)}\frac{\xi_i - x_i}{3}$ are the barycentric coordinates of the point $\frac{2}{3}x_i + \frac{1}{3}\xi_i$ w.r.t. W_i, which implies that they are also the barycentric coordinates of the point ξ_i w.r.t. the interval $[x_{i-1},\ x_{i+1}]$. Hence, throughout multi-affinity of the blossom and by (12), one can obtain

$$\mathcal{B}\left[\mathcal{Q}f_{|J_{i,1}}\right](x_i[2],\ \xi_i) = \mathcal{B}\left[\mathcal{I}^{\mathrm{kn}}_{i,(\ell,m)}f\right](x_i[2],\ \xi_i) = \mathcal{B}[p](x_i[2],\ \xi_i).$$

Considering the B-ordinate of $\mathcal{Q}f_{|J_{i,1}}$ corresponding to the domain point $\frac{1}{3}x_i + \frac{2}{3}\xi_i$, it holds

$$\mathcal{B}\left[\mathcal{Q}f_{|J_{i,1}}\right](\xi_i[3]) = \tau^2_{i,1}\mathcal{B}\left[\mathcal{Q}f_{|J_{i,1}}\right](x_i[2], \xi_i) + 2\tau_{i,1}\tau_{i,2}\mathcal{B}\left[\mathcal{Q}f_{|J_{i,1}}\right](x_i, x_{i+1}, \xi_i) + \tau^2_{i,2}\mathcal{B}\left[\mathcal{Q}f_{|J_{i,1}}\right](x_{i+1}[2], \xi_i)$$

and

$$\mathcal{B}\left[\mathcal{Q}f_{|J_{i,1}}\right](x_i, x_{i+1}, \xi_i) = \frac{-\tau_{i,1}}{\tau_{i,2}}\mathcal{B}\left[\mathcal{Q}f_{|J_{i,1}}\right](x_i[2], \xi_i) + \frac{1}{\tau_{i,2}}\mathcal{B}\left[\mathcal{Q}f_{|J_{i,1}}\right](x_i, \xi_i[2]),$$

so that

$$\mathcal{B}\left[\mathcal{Q}f_{|J_{i,1}}\right](x_i, \xi_i[2]) = \frac{\tau_{i,1}}{2}\mathcal{B}\left[\mathcal{Q}f_{|J_{i,1}}\right](x_i[2], \xi_i) + \frac{1}{2\tau_{i,1}}\mathcal{B}\left[\mathcal{Q}f_{|J_{i,1}}\right](\xi_i[3]) - \frac{\tau^2_{i,2}}{2\tau_{i,1}}\mathcal{B}\left[\mathcal{Q}f_{|J_{i,1}}\right](x_{i+1}[2], \xi_i).$$

From (13), we get

$$\begin{aligned} \mathcal{B}\left[\mathcal{Q}f_{|J_{i,1}}\right](x_i,\ \xi_i[2]) &= \frac{\tau_{i,1}}{2}\mathcal{B}[p](x_i[2], \xi_i) + \frac{1}{2\tau_{i,1}}p(\xi_i) - \frac{\tau^2_{i,2}}{2\tau_{i,1}}\mathcal{B}[p](x_{i+1}[2], \xi_i) \\ &= \mathcal{B}[p](x_i,\ \xi_i[2]), \end{aligned}$$

This proves that $\lim_{x\to x_i, x>x_i}(Qf)''(x) = p''(x_i)$. It only remains to prove that $\lim_{x\to x_i, x<x_i}(Qf)''(x) = p''(x_i)$. By the same approach used for the right case, the blossom value $\mathcal{B}\left[\mathcal{Q}f_{|J_{i-1,2}}\right](x_i[2], \xi_i)$ is the B-ordinate of $\mathcal{Q}f_{|J_{i-1,2}}$ on $J_{i-1,2}$ corresponding to the domain point $\frac{2}{3}x_i + \frac{1}{3}\xi_{i-1}$(9), i.e.

$$\mathcal{B}\left[\mathcal{Q}f_{|J_{i-1,2}}\right](x_i[2],\ \xi_{i-1}) = \sum_{\ell+m=1}\left(\alpha_{i,(\ell,m)} + \beta_{i,(\ell,m)}\frac{x_i - \xi_{i-1}}{3}\right)\mathcal{B}\left[\mathcal{I}^{\mathrm{kn}}_{i,(\ell,m)}f\right](x_i[2],\ x_{i-1}[\ell],\ x_{i+1}[m]).$$

In this case, the weights $\alpha_{i,(\ell,m)} + \beta_{i,(\ell,m)}\frac{x_i - \xi_{i-1}}{3}$ relative to the barycentric coordinates of point $\frac{2}{3}x_i + \frac{1}{3}\xi_{i-1}$ w.r.t. W_i, which implies that they are also the barycentric coordinates of point ξ_{i-1} w.r.t. the interval $[x_{i-1},\ x_{i+1}]$. By using (12), one gets

$$\mathcal{B}\left[\mathcal{Q}f_{|J_{i-1,2}}\right](x_i[2],\ \xi_{i-1}) = \mathcal{B}\left[\mathcal{I}^{\mathrm{kn}}_{i,(\ell,m)}f\right](x_i[2],\ \xi_{i-1}) = \mathcal{B}[p](x_i[2],\ \xi_{i-1}).$$

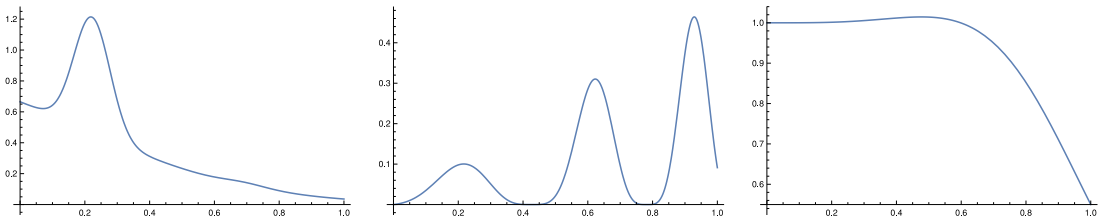

Fig. 5. Plots of tests functions: f_1 (left), f_2 (center) and f_3 (right).

Considering the condition (14) corresponding to the interval I_{i-1}, i.e., $\mathcal{I}^{\mathrm{sp}}_{i-1} f\left(\xi_{i-1}\right) = p\left(\xi_{i-1}\right)$, the blossom $\mathcal{B}\left[\mathcal{Q}f_{|J_{i-1,2}}\right]\left(x_i, \xi_{i-1}[2]\right)$ can be expressed as follows:

$$\begin{aligned}\mathcal{B}\left[\mathcal{Q}f_{|J_{i-1,2}}\right]\left(x_i,\ \xi_{i-1}[2]\right) &= \frac{\tau_{i-1,1}}{2}\mathcal{B}[p]\left(x_{i-1}[2], \xi_{i-1}\right) + \frac{1}{2\tau_{i-1,1}} p\left(\xi_{i-1}\right) - \frac{\tau^2_{i-1,2}}{2\tau_{i-1,1}}\mathcal{B}[p]\left(x_i[2], \xi_{i-1}\right)\\ &= \mathcal{B}[p]\left(x_i,\ \xi_{i-1}[2]\right).\end{aligned}$$

This confirms that $(\mathcal{Q}f)''(x_i) = p''(x_i)$. □

Next, we provide a rule to choose the operators $\mathcal{I}^{\mathrm{kn}}_{i,(\ell,m)}$ and $\mathcal{I}^{\mathrm{sp}}_k$ in such a way that the conditions in Theorem 2 are fulfilled.

For each $0 \le i \le n$, let $\mathcal{I}^{\mathrm{kn}}_i f$ be the cubic polynomial such that

$$\mathcal{I}^{\mathrm{kn}}_i f(x_i) = f(x_i), \quad \mathcal{I}^{\mathrm{kn}}_i f'(x_i) = f'(x_i), \quad \mathcal{I}^{\mathrm{kn}}_i f(\xi_{i-1}) = f(\xi_{i-1}) \text{ and } \mathcal{I}^{\mathrm{kn}}_i f(\xi_i) = f(\xi_i),$$

and $\mathcal{Q}f$ be defined by (10).

- For every knot x_i, take $\mathcal{I}^{\mathrm{kn}}_{i,(\ell,m)} f = \mathcal{I}^{\mathrm{kn}}_i f$, $\ell + m = 1$.
- Take $\mathcal{I}^{\mathrm{sp}}_k f = \mathcal{I}^{\mathrm{kn}}_k f$, where $\mathcal{I}^{\mathrm{kn}}_k f$ is associated with x_k, which is the first end-point of I_k.

These choices ensure that $\mathcal{Q}f \in S^2_3\left(\widetilde{X}_n\right)$. Approaches to get bivariate C^2 cubic splines on a 6-split have been discussed in [33].

3.3. Numerical results

This section provides some numerical results to illustrate the performance of the above quasi-interpolation operators. To this end, we will use the test functions

$$\begin{aligned}f_1(x) &= \frac{3}{4}e^{-2(9x-2)^2} - \frac{1}{5}e^{-(9x-7)^2-(9x-4)^2} + \frac{1}{2}e^{-(9x-7)^2-\frac{1}{4}(9x-3)^2} + \frac{3}{4}e^{\frac{1}{10}(-9x-1)-\frac{1}{49}(9x+1)^2},\\ f_2(x) &= \frac{1}{2}x\cos^4\left(4\left(x^2+x-1\right)\right),\\ f_3(x) &= x^4e^{-3x^2} + \frac{1}{x^6+1},\end{aligned}$$

whose plots appear in Fig. 5. The two first functions are the 1D versions of Franke [34] and Nielson [35] functions.

Let us consider the interval $I = [0, 1]$. The tests are carried out for a sequence of uniform mesh X_n associated with the knots $x_i = ih$, $i = 0, \ldots, n$, where $h = \frac{1}{n}$. The inserted split points are chosen as the middle points of the macro-intervals, i.e., $\xi_i = \left(i + \frac{1}{2}\right)h$, $i = 0, \ldots, n-1$.

For each $i = 0, \ldots, n$, we have

$$\begin{aligned}\mathcal{I}^{\mathrm{kn}}_i f(x) = f\left(\xi_{i-1}\right)\mathfrak{B}^3_{(3,0),[\xi_{i-1},\xi_i]} &+ \frac{1}{3}\left(2\left(\xi_{i-1}-\xi_i\right)f'\left(x_i\right) - 2f\left(\xi_{i-1}\right) + f\left(\xi_i\right) + 4f\left(x_i\right)\right)\mathfrak{B}^3_{(2,1),[\xi_{i-1},\xi_i]}\\ &+ \frac{1}{3}\left(2\left(\xi_i-\xi_{i-1}\right)f'\left(x_i\right) + f\left(\xi_{i-1}\right) - 2f\left(\xi_i\right) + 4f\left(x_i\right)\right)\mathfrak{B}^3_{(1,2),[\xi_{i-1},\xi_i]} + f\left(\xi_i\right)\mathfrak{B}^3_{(0,3),[\xi_{i-1},\xi_i]}.\end{aligned}$$

It interpolates the value and the first derivative value of f at x_i and the function values of f at ξ_{i-1} and ξ_i.

From this choice, the linear functionals $\psi^{\mathrm{kn}}_{i,(\ell,m)}$ and ψ^{sp}_k will be given by the following expressions:

$$\begin{aligned}\psi^{\mathrm{kn}}_{i,(1,0)}(f) &= f\left(\frac{i}{n}\right) - \frac{2}{3n}f'\left(\frac{i}{n}\right),\\ \psi^{\mathrm{kn}}_{i,(0,1)}(f) &= f\left(\frac{i}{n}\right) + \frac{2}{3n}f'\left(\frac{i}{n}\right),\end{aligned}$$

Table 1
Estimated errors for functions f_1, f_2 and f_3, and NCOs with different values of n.

n	$\mathcal{E}_n(f_1)$	NCO	$\mathcal{E}_n(f_2)$	NCO	$\mathcal{E}_n(f_3)$	NCO
16	3.2851×10^{-3}	–	8.3227×10^{-3}	–	6.5942×10^{-6}	–
32	3.8209×10^{-4}	3.10	5.1442×10^{-4}	4.01	4.1899×10^{-7}	3.97
64	2.1478×10^{-5}	4.15	2.9507×10^{-5}	4.12	2.5085×10^{-8}	4.06
128	9.9300×10^{-7}	4.43	1.8595×10^{-6}	3.98	1.4689×10^{-9}	4.09
256	7.5323×10^{-8}	3.72	1.1592×10^{-7}	4.00	9.9866×10^{-11}	3.87

Table 2
Quasi-interpolation errors and NCOs for the test function g_1 with different values of n.

n	$\mathcal{E}_n(g_1)$	NCO	Method in [36]	NCO
16	2.1352×10^{-8}	–	3.25116×10^{-7}	–
32	1.3627×10^{-9}	3.96	2.13504×10^{-8}	3.92862
64	8.6021×10^{-11}	3.98	1.36452×10^{-9}	3.96779
128	5.4025×10^{-12}	3.99	8.61907×10^{-11}	3.98472

Table 3
Quasi-interpolation errors and NCOs for the test function g_2 with different values of n.

n	$\mathcal{E}_n(g_2)$	NCO	Method in [37]	NCO
64	2.1282×10^{-7}	–	4.11124×10^{-6}	–
128	1.3140×10^{-8}	4.01	2.59629×10^{-7}	3.98505
256	7.3024×10^{-10}	4.16	1.62327×10^{-8}	3.99948
512	5.2902×10^{-11}	3.78	1.01501×10^{-9}	3.99934

$$\psi_i^{\mathrm{sp}}(f) = \frac{1}{2n} f'\left(\frac{i}{n}\right) + \frac{1}{3}\left(f\left(\frac{2i-1}{2n}\right) + f\left(\frac{i}{n}\right) + f\left(\frac{2i+1}{2n}\right)\right).$$

The quasi-interpolation error is estimated as

$$\mathcal{E}_n(f) = \max_{0\le \ell \le 200} |\mathcal{Q}f(z_\ell) - f(z_\ell)|, \tag{15}$$

where z_ℓ, $\ell = 0, \ldots, 200$, are equally spaced points in I. The estimated numerical convergence order (NCO) is given by the rate

$$NCO := \frac{\log\left(\frac{\mathcal{E}_{n_1}}{\mathcal{E}_{n_2}}\right)}{\log\left(\frac{n_2}{n_1}\right)}.$$

In Table 1, the estimated quasi-interpolation errors and NCOs for functions f_1, f_2 and f_3 are shown.

In what follows, a comparison between the numerical results obtained by the proposed C^2 cubic spline quasi-interpolating scheme and the results presented in [36,37] is done. In them, the following test functions are considered:

$$g_1(x) = \sin x, \quad \text{and} \quad g_2(x) = -\frac{1}{2}\left(\exp\left(\frac{x^3}{2}\right) - 1\right)\cos(3\pi x).$$

In Tables 2 and 3, we list the resulting errors and NCOs for the approximation of functions g_1 and g_2, respectively, by using the cubic spline quasi-interpolant proposed here and those in [36,37]. The proposed scheme improves the results in those papers by two orders of magnitude.

4. Spline spaces on twice-refined partitions

In the previous section a C^2 cubic quasi-interpolant on a refinement $\widetilde{X}_n$ of the initial partition X_n by adding an additional knot at each macro-interval has been defined. That quasi-interpolant is written in terms of B-spline-like functions $\mathcal{D}^{\mathrm{kn}}_{i,(\ell,m)}$, $0 \le i \le n$, $\ell + m = 1$, and $\mathcal{D}^{\mathrm{sp}}_k$, $0 \le k \le n-1$.

Let $\widetilde{X}_{n,2}$ be the refinement of the refined partition $\widetilde{X}_{n,1} := \widetilde{X}_n$ produced in decomposing each sub-interval in $\widetilde{X}_{n,1}$ into two micro-intervals by inserting points $\xi_{i,1}$ and $\xi_{i,2}$ into $\widetilde{I}_{i,1} := [x_i, \xi_i]$ and $\widetilde{I}_{i,2} := [\xi_i, x_{i+1}]$, respectively. The sub-space $S_3^2\left(\widetilde{X}_{n,1}\right)$ of $S_3^{1,2}\left(\widetilde{X}_{n,1}\right)$ is refinable under the refinement $\widetilde{X}_{n,2}$, i.e., a spline $s \in S_3^2\left(\widetilde{X}_{n,1}\right)$ is also an element of the finer space $S_3^2\left(\widetilde{X}_{n,2}\right)$. The computation of such a spline by refinement of the original refined partition, while retaining the cubic precision, is considered in this section. Indeed, we aim to express a spline s expressed as in (5) using the same kind of representation but with respect to $S_3^2\left(\widetilde{X}_{n,2}\right)$. The coefficients related with the finer partition $\widetilde{X}_{n,2}$ are written in terms of coefficients $c^{\mathrm{kn}}_{i,(\ell,m)}$ and c^{sp}_k associated with the partition $\widetilde{X}_{n,1}$. The subdivision rules presented in this section are valid for

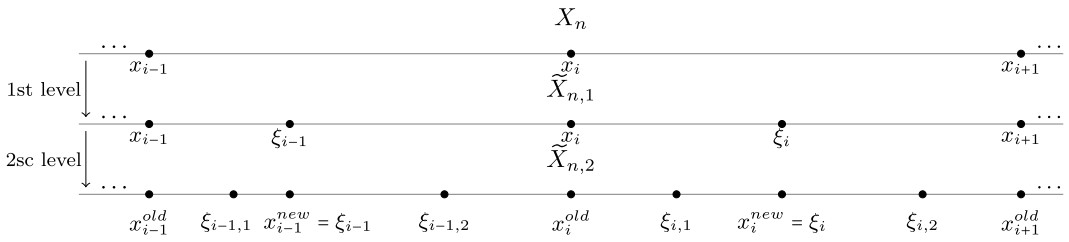

Fig. 6. A schematic representation for the initial (top), first (center) and second refinement (bottom) levels.

any spline $s \in S_3^{1,2}\left(\widetilde{X}_{n,1}\right)$, which implies that, the proposed subdivision rules produce splines of the same regularity as the initial ones.

The elements of the initial partition X_n are noted using the term "x", while the elements of $\widetilde{X}_{n,1}$ are noted by "x" and "ξ", referring to the initial and new inserted knots, respectively. Consequently, for each level, two different notations are used, namely "x" for the old knots and "ξ" for the new inserted ones. For this reason, we will keep the same strategy for $\widetilde{X}_{n,2}$, i.e. the induced element of $\widetilde{X}_{n,1}$ will be named using the term "x" and "ξ" for the new inserted knots. The induced elements of $\widetilde{X}_{n,1}$ are x_i, $i = 0, \ldots, n$ and ξ_i, $i = 0, \ldots, n-1$, these elements are the initial elements of $\widetilde{X}_{n,2}$, so the following notation will be adopted: $x_i^{\text{old}} := x_i$ and $x_i^{\text{new}} = \xi_i$. A schematic representation of the two levels of refinement is depicted in Fig. 6.

The spline space $S_3^2\left(\widetilde{X}_{n,1}\right)$ is considered since we are interested in refining C^2 cubic functions, namely the quasi-interpolants constructed in the previous section. The space $S_3^2\left(\widetilde{X}_{n,2}\right)$ is also involved. A spline $s \in S_3^2\left(\widetilde{X}_{n,1}\right)$ is also an element of the finer space $S_3^2\left(\widetilde{X}_{n,2}\right)$, and we look for expressing the coefficients in (5) associated with second level partition $\widetilde{X}_{n,2}$ in terms of those corresponding to the first level refinement $\widetilde{X}_{n,1}$.

Le us suppose that the spline $s \in S_3^2\left(\widetilde{X}_{n,2}\right)$ is expressed as

$$s = \sum_{i=0}^{n} \sum_{\ell+m=1} c_{i,(\ell,m)}^{\text{kn, old}}\, \mathcal{D}_{i,(\ell,m)}^{\text{kn, old}} + \sum_{i=0}^{n} \sum_{\ell+m=1} c_{i,(\ell,m)}^{\text{kn, new}}\, \mathcal{D}_{i,(\ell,m)}^{\text{kn, new}} + \sum_{k=0}^{n-1} \left(c_k^{\text{sp},1}\, \mathcal{D}_k^{\text{sp},1} + c_k^{\text{sp},2}\, \mathcal{D}_k^{\text{sp},2} \right), \tag{16}$$

where $c_{i,(\ell,m)}^{\text{kn, old}}$, $c_{i,(\ell,m)}^{\text{kn, new}}$, $c_k^{\text{sp},1}$ and $c_k^{\text{sp},2}$ are the coefficients associated with points x_i^{old}, x_i^{new}, $\xi_{k,1}$ and $\xi_{k,2}$, respectively.

We will start by providing the expressions of the spline coefficients associated with a uniform partition, where the inserted split points in each level are the mid-points. Later on, we will prove subdivision rules for the case of non-uniform partitions.

4.1. Subdivision rules for uniform partitions

Consider the uniform case, with $x_i = a + ih$, $i = 0, \ldots, n$, h being the step-size. In this case, the inserted split points in the first level are $\xi_i = \frac{1}{2}(x_i + x_{i+1})$, and those corresponding to the second level refinement are $\xi_{i,1} = \frac{3}{4}x_i + \frac{1}{4}x_{i+1}$ and $\xi_{i,2} = \frac{1}{4}x_i + \frac{3}{4}x_{i+1}$.

The following results show the relationship between old and new coefficients for knots.

Proposition 3. *The coefficients $c_{i,(\ell,m)}^{kn,old}$, $\ell + m = 1$, corresponding to the knot x_i^{old} are expressed as*

$$c_{i,(1,0)}^{kn,\ old} = \frac{3}{4}c_{i,(1,0)}^{kn} + \frac{1}{4}c_{i,(0,1)}^{kn}, \qquad c_{i,(0,1)}^{kn,\ old} = \frac{1}{4}c_{i,(1,0)}^{kn} + \frac{3}{4}c_{i,(0,1)}^{kn}.$$

Proof. Let L be a sub-interval of $\widetilde{X}_{n,2}$ with an end-point at x_i. Note that $x_i^{\text{new}} = \xi_i = \frac{3}{4}x_i + \frac{1}{4}x_{i+2}$. Then, using the multi-affinity of blossoms and (7), we have

$$\begin{aligned} c_{i,(1,0)}^{\text{kn, old}} &= \mathcal{B}\left[s_{|L}\right]\left(x_i^{\text{old}}[2],\ x_{i-1}^{\text{new}}\right) \\ &= \mathcal{B}\left[s_{|L}\right]\left(x_i[2],\ \frac{3}{4}x_{i-1} + \frac{1}{4}x_{i+1}\right) \\ &= \frac{3}{4}\mathcal{B}\left[s_{|L}\right](x_i[2],\ x_{i-1}) + \frac{1}{4}\mathcal{B}\left[s_{|L}\right](x_i[2],\ x_{i+1}), \end{aligned}$$

and,

$$\begin{aligned} c^{\text{kn, old}}_{i,(0,1)} &= \mathcal{B}\left[s_{|L}\right]\left(x_i^{\text{old}}[2]\,,\ x_{i+1}^{\text{new}}\right)\\ &= \mathcal{B}\left[s_{|L}\right]\left(x_i[2]\,,\ \frac{1}{4}x_{i-1}+\frac{3}{4}x_{i+1}\right)\\ &= \frac{1}{4}\mathcal{B}\left[s_{|L}\right](x_i[2]\,,\ x_{i-1})+\frac{3}{4}\mathcal{B}\left[s_{|L}\right](x_i[2]\,,\ x_{i+1})\,, \end{aligned}$$

$s_{|L}$ stands for the restriction of s to L. The proof is complete. □

Proposition 4. *The coefficients $c^{kn,new}_{i,(\ell,m)}$, $\ell+m=1$, corresponding to the knot x_i^{new} are expressed as*

$$c^{kn,\ new}_{i,(1,0)} = \frac{1}{8}c^{kn}_{i,(1,0)}+\frac{3}{8}c^{kn}_{i,(0,1)}+\frac{1}{2}c_i^{sp}, \qquad c^{kn,\ new}_{i,(0,1)} = \frac{3}{8}c^{kn}_{i+1,(1,0)}+\frac{1}{8}c^{kn}_{i+1,(0,1)}+\frac{1}{2}c_i^{sp}.$$

Proof. Let L be a sub-interval of $\widetilde{X}_{n,2}$ with an end-point at x_i^{new}. Again, we use the multi-affinity of blossoms and (7) –(8) to get

$$\begin{aligned} c^{\text{kn, new}}_{i,(1,0)} &= \mathcal{B}\left[s_{|L}\right]\left(x_i^{\text{new}}[2]\,,\ x_i^{\text{old}}\right)\\ &= \frac{1}{2}\mathcal{B}\left[s_{|L}\right]\left(x_i^{\text{new}},\ x_i^{\text{old}}[2]\right)+\frac{1}{2}\mathcal{B}\left[s_{|L}\right]\left(x_i^{\text{new}},\ x_i^{\text{old}},\ x_{i+1}^{\text{old}}\right)\\ &= \frac{1}{2}\left(\frac{1}{4}\mathcal{B}\left[s_{|L}\right](x_i[2]\,,\ x_{i-1})+\frac{3}{4}\mathcal{B}\left[s_{|L}\right](x_i[2]\,,\ x_{i+1})\right)+\frac{1}{2}\mathcal{B}\left[s_{|L}\right](\xi_i,\ x_i,\ x_{i+1})\,. \end{aligned}$$

The same technique is used to get the expression of $c^{\text{kn, new}}_{i,(0,1)}$. □

Similar results are given next for split points.

Proposition 5. *The coefficients $c_i^{sp,1}$ and $c_i^{sp,2}$ associated with the split points $\xi_{i,1}$ and $\xi_{i,2}$, respectively, are given by*

$$c_i^{sp,1} = \frac{3}{16}c^{kn}_{i,(1,0)}+\frac{9}{16}c^{kn}_{i,(0,1)}+\frac{1}{4}c_i^{sp}, \qquad c_i^{sp,2} = \frac{9}{16}c^{kn}_{i+1,(1,0)}+\frac{3}{16}c^{kn}_{i+1,(0,1)}+\frac{1}{4}c_i^{sp}.$$

Proof. Let L be a sub-interval of $\widetilde{X}_{n,2}$ with an end-point at $\xi_{i,1}$. Using (8), we can write

$$c_i^{\text{sp},1} = \mathcal{B}\left[s_{|L}\right]\left(\xi_{i,1},\ x_i^{\text{old}},\ x_i^{\text{new}}\right).$$

By definition, $\xi_{i,1} = \frac{1}{2}x_i^{\text{old}}+\frac{1}{2}x_i^{\text{new}}$ and

$$x_i^{\text{new}} = \frac{1}{2}x_i^{\text{old}}+\frac{1}{2}x_{i+1}^{\text{old}} = \frac{1}{4}x_{i-1}^{\text{old}}+\frac{3}{4}x_{i+1}^{\text{old}}.$$

Then, by multi-affinity of blossoms, we have

$$c_i^{\text{sp},1} = \frac{1}{2}\mathcal{B}\left[s_{|L}\right]\left(x_i^{\text{old}}[2],\ x_i^{\text{new}}\right)+\frac{1}{2}\mathcal{B}\left[s_{|L}\right]\left(x_i^{\text{old}},\ x_i^{\text{new}}[2]\right).$$

Taking into account that

$$\begin{aligned} \mathcal{B}\left[s_{|L}\right]\left(x_i^{\text{old}}[2],\ x_i^{\text{new}}\right) &= \frac{1}{4}\mathcal{B}\left[s_{|L}\right]\left(x_i^{\text{old}}[2],\ x_{i-1}^{\text{old}}\right)+\frac{3}{4}\mathcal{B}\left[s_{|L}\right]\left(x_i^{\text{old}}[2],\ x_{i+1}^{\text{old}}\right)\\ &= \frac{1}{4}c^{\text{kn}}_{i,(1,0)}+\frac{3}{4}c^{\text{kn}}_{i,(0,1)} \end{aligned}$$

and

$$\begin{aligned} \mathcal{B}\left[s_{|L}\right]\left(x_i^{\text{old}},\ x_i^{\text{new}}[2]\right) &= \frac{1}{2}\mathcal{B}\left[s_{|L}\right]\left(x_i^{\text{old}}[2],\ x_i^{\text{new}}\right)+\frac{1}{2}\mathcal{B}\left[s_{|L}\right]\left(x_i^{\text{old}},\ x_{i+1}^{\text{old}},\ x_i^{\text{new}}\right)\\ &= \frac{1}{8}c^{\text{kn}}_{i,(1,0)}+\frac{3}{8}c^{\text{kn}}_{i,(0,1)}+\frac{1}{4}c_i^{\text{sp}}, \end{aligned}$$

the claim follows for $c_i^{\text{sp},1}$. The same approach is used to prove the expression for $c_i^{\text{sp},2}$. □

4.2. Subdivision rules for non-uniform partition

Now, we consider the case of non-uniform partitions. Let

$$\mathbb{B}_i^n[a,b,c] = \binom{n}{i}\frac{(b-c)^i(c-a)^{n-i}}{(b-a)^n}$$

be the ith Bernstein basis function of degree n w.r.t. $[a, b]$ (note that the Bernstein basis functions in (1) are expressed in terms of barycentric coordinates w.r.t. $[a, b]$). Let L^{o}, L^{n} and L^{sp} be sub-intervals of $\widetilde{X}_{n,2}$ with end-points at x_i^{old}, x_i^{new} and $\xi_{i,1}$, respectively. Then, the following results are obtained.

1. Subdivision rules for the coefficients associated with the set of old knots: for $\ell + m = 1$,

$$\begin{aligned} c^{\mathrm{kn,\ old}}_{i,(\ell,m)} &= \mathcal{B}[s_{|L^{\mathrm{o}}}]\left(x_i^{\mathrm{old}}[r+1], x_{i-1}^{\mathrm{new}}[\ell], x_i^{\mathrm{new}}[m]\right), \\ &= \sum_{j=0}^{l}\sum_{k=0}^{m} \mathbb{B}_j^{\ell}\left[x_{i-1}^{\mathrm{old}}, x_{i+1}^{\mathrm{old}}, x_{i-1}^{\mathrm{new}}\right] \mathbb{B}_k^{m}\left[x_{i-1}^{\mathrm{old}}, x_{i+1}^{\mathrm{old}}, x_i^{\mathrm{new}}\right] \\ &\times \mathcal{B}\left[s_{|L^{\mathrm{o}}}\right]\left(x_i^{\mathrm{old}}[r+1], x_{i-1}^{\mathrm{old}}[j+k], x_{i+1}^{\mathrm{old}}[r-j-k]\right), \\ &= \sum_{j=0}^{l}\sum_{k=0}^{m} \mathbb{B}_j^{\ell}\left[x_{i-1}^{\mathrm{old}}, x_{i+1}^{\mathrm{old}}, x_{i-1}^{\mathrm{new}}\right] \mathbb{B}_k^{m}\left[x_{i-1}^{\mathrm{old}}, x_{i+1}^{\mathrm{old}}, x_i^{\mathrm{new}}\right] c^{\mathrm{kn}}_{i,(j+k,r-j-k)}. \end{aligned}$$

2. Subdivision rules for the coefficients associated with the set of new knots:

- For $\ell = 1$ and $m = 0$,

$$\begin{aligned} c^{\mathrm{kn,\ new}}_{i,(1,0)} &= \mathcal{B}\left[s_{|L^{\mathrm{n}}}\right]\left(x_i^{\mathrm{new}}[2], x_i^{\mathrm{old}}\right), \\ &= \mathbb{B}_0^1\left[x_i^{\mathrm{old}}, x_{i+1}^{\mathrm{old}}, x_i^{\mathrm{new}}\right] \mathcal{B}\left[s_{|L^{\mathrm{n}}}\right]\left(x_i^{\mathrm{new}}, x_i^{\mathrm{old}}[2]\right) \\ &+ \mathbb{B}_1^1\left[x_i^{\mathrm{old}}, x_{i+1}^{\mathrm{old}}, x_i^{\mathrm{new}}\right] \mathcal{B}\left[s_{|L^{\mathrm{n}}}\right]\left(x_i^{\mathrm{new}}, x_i^{\mathrm{old}}, x_{i+1}^{\mathrm{old}}\right), \\ &= \mathbb{B}_0^1\left[x_i^{\mathrm{old}}, x_{i+1}^{\mathrm{old}}, x_i^{\mathrm{new}}\right] \sum_{j=0}^{1} \mathbb{B}_j^1\left[x_{i-1}^{\mathrm{old}}, x_{i+1}^{\mathrm{old}}, x_i^{\mathrm{new}}\right] c^{\mathrm{kn}}_{i,(j,1-j)} \\ &+ \mathbb{B}_1^1\left[x_i^{\mathrm{old}}, x_{i+1}^{\mathrm{old}}, x_i^{\mathrm{new}}\right] c_i^{\mathrm{sp}}. \end{aligned}$$

- For $\ell = 0$ and $m = 1$,

$$\begin{aligned} c^{\mathrm{kn,\ new}}_{i,(0,1)} &= \mathcal{B}\left[s_{|L^{\mathrm{n}}}\right]\left(x_i^{\mathrm{new}}[2], x_{i+1}^{\mathrm{old}}\right), \\ &= \mathbb{B}_0^1\left[x_i^{\mathrm{old}}, x_{i+1}^{\mathrm{old}}, x_i^{\mathrm{new}}\right] c_i^{\mathrm{sp}} \\ &+ \mathbb{B}_1^1\left[x_i^{\mathrm{old}}, x_{i+1}^{\mathrm{old}}, x_i^{\mathrm{new}}\right] \sum_{j=0}^{1} \mathbb{B}_j^1\left[x_i^{\mathrm{old}}, x_{i+2}^{\mathrm{old}}, x_i^{\mathrm{new}}\right] c^{\mathrm{kn}}_{i+1,(j,1-j)}. \end{aligned}$$

3. Subdivision rules for the coefficients associated with the set of split points (we consider only the subdivision rule associated with $\xi_{i,1}$, the case of $\xi_{i,2}$ being similar): it holds

$$\begin{aligned} c_i^{\mathrm{sp},1} &= \mathcal{B}\left[s_{|L^{\mathrm{sp}}}\right]\left(\xi_{i,1}, x_i^{\mathrm{old}}, x_i^{\mathrm{new}}\right), \\ &= \sum_{j=0}^{1} \mathbb{B}_j^1\left[x_i^{\mathrm{old}}, x_i^{\mathrm{new}}, \xi_{i,1}\right] \mathcal{B}\left[s_{|L^{\mathrm{sp}}}\right]\left(x_i^{\mathrm{old}}[1+j], x_i^{\mathrm{new}}[2-j]\right), \\ &= \mathbb{B}_0^1\left[x_i^{\mathrm{old}}, x_i^{\mathrm{new}}, \xi_{i,1}\right] \Xi_1 + \mathbb{B}_1^1\left[x_i^{\mathrm{old}}, x_i^{\mathrm{new}}, \xi_{i,1}\right] \Xi_2, \end{aligned}$$

where

$$\Xi_1 := \mathbb{B}_0^1\left[x_i^{\mathrm{old}}, x_{i+1}^{\mathrm{old}}, x_i^{\mathrm{new}}\right] c_i^{\mathrm{sp}} + \mathbb{B}_1^1\left[x_i^{\mathrm{old}}, x_{i+1}^{\mathrm{old}}, x_i^{\mathrm{new}}\right] \sum_{q=0}^{1} \mathbb{B}_q^1\left[x_{i-1}^{\mathrm{old}}, x_{i+1}^{\mathrm{old}}, x_i^{\mathrm{new}}\right] c^{\mathrm{kn}}_{i,(q,1-q)}$$

and

$$\Xi_2 := \sum_{q=0}^{1} \mathbb{B}_q^1\left[x_{i-1}^{\mathrm{old}}, x_{i+1}^{\mathrm{old}}, x_i^{\mathrm{new}}\right] c^{\mathrm{kn}}_{i,(q,1-q)}.$$

4.3. Numerical examples

The results obtained in the previous subsections provide a set of subdivision rules that can be applied for representing a spline in $S_3^{1,2}\left(\widetilde{X}_{n,1}\right)$ in terms of the B-splines of the finer space $S_3^{1,2}\left(\widetilde{X}_{n,2}\right)$. Those rules involve non-negative weights, and the B-spline coefficients associated with the finer space $S_3^{1,2}\left(\widetilde{X}_{n,2}\right)$ are computed as convex combinations of the B-spline coefficients associated with the space $S_3^{1,2}\left(\widetilde{X}_{n,1}\right)$, which gives an efficient visualization tool.

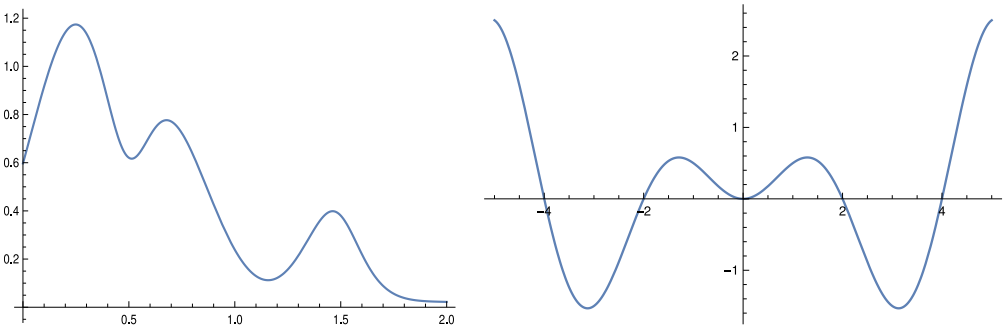

Fig. 7. From left to right, plots of h_1 and h_2.

For $i = 0, \ldots, n$, and $k = 0, \ldots, n-1$, define the control points

$$\mathbf{c}^{\mathrm{kn}}_{i,(1,0)} := \left(W_{i,1},\ c^{\mathrm{kn}}_{i,(1,0)}\right), \quad \mathbf{c}^{\mathrm{kn}}_{i,(0,1)} := \left(W_{i,2},\ c^{\mathrm{kn}}_{i,(0,1)}\right), \quad \mathbf{c}^{\mathrm{sp}}_{k} := \left(\frac{1}{3}\xi_k + \frac{1}{3}\left(x_k + x_{k+1}\right),\ c^{\mathrm{sp}}_{k}\right), \tag{17}$$

where $c^{\mathrm{kn}}_{i,(1,0)}$, $c^{\mathrm{kn}}_{i,(0,1)}$ and c^{sp}_{k} are the B-spline coefficients in the representation (5), $W_{i,j}$, $j = 1, 2$, are defined in (6) and $Z_k := \frac{1}{3}\xi_k + \frac{1}{3}\left(x_k + x_{k+1}\right)$. It holds

$$x = \sum_{i=0}^{n}\left(W_{i,1}\mathcal{D}^{\mathrm{kn}}_{i,(1,0)}(x) + W_{i,2}\mathcal{D}^{\mathrm{kn}}_{i,(0,1)}(x)\right) + \sum_{k=0}^{n-1} Z_k\,\mathcal{D}^{\mathrm{sp}}_{k}(x).$$

A full proof is given in [7]. The restriction of a spline given by (5) to each macro-interval reduces to a sum involving only five B-splines and their corresponding control points given in (17). Therefore, the graph of such a restriction lies in the convex hull determined by those five control points. From the fact that the B-spline basis is a convex partition of unity, the whole graph of the spline lies in the union of the resulting convex hulls. This is a property well appreciated in CAGD.

In what follows, we will show the performance of the subdivision rules obtained by applying them to the interpolation splines provided by Theorem 1 in the space $S_3^{1,2}\left(\widetilde{X}_{n,1}\right)$ for two test functions. They are

$$h_1(x) = \frac{\exp\left(-x^2\right)\left(\log\left(x^5+6\right) + \sin(3\pi x)\right)}{\cos(2\pi x) + 2} \quad \text{and} \quad h_2(x) = x\sin\frac{\pi}{2}x.$$

For h_1, we take $I = [0, 2]$ and $n = 10$, while $I = [-4, 4]$ and $n = 16$ for h_2. Therefore control polygons with few control points are obtained. Their plots are shown in Fig. 7. In both cases, we will work with uniform partitions of the above intervals. In each interval induced by the partition, the inserted point is the mid-point of the interval.

The rules to be applied become

$$\begin{aligned}
c^{\mathrm{kn}}_{i,(1,0)} &= s(x_i) + \frac{2}{3}h\,s'(x_i),\\
c^{\mathrm{kn}}_{i,(0,1)} &= s(x_i) - \frac{2}{3}h\,s'(x_i),\\
c^{sp}_{k} &= 2\,s(\xi_k) - \frac{1}{16}\left(3c^{\mathrm{kn}}_{k,(1,0)} + 5c^{\mathrm{kn}}_{k,(0,1)} + 5c^{\mathrm{kn}}_{k+1,(1,0)} + 3c^{\mathrm{kn}}_{k+1,(0,1)}\right),
\end{aligned}$$

h being the step-length of the partition.

By applying some steps of the proposed subdivision rules, the resulting control polygons should converge to the function curve. In Fig. 8, the results provided by the subdivision rules applied to the initial control polygon for function h_1 are shown. They are associated with partitions $\widetilde{X}_{10,1}$, $\widetilde{X}_{10,2}$, $\widetilde{X}_{10,3}$, and $\widetilde{X}_{10,4}$. Fig. 8 shows how control polygons are produced closer and closer to the graph of h_1.

Fig. 9 shows the results of applying the subdivision rules to the control polygon of the curve of h_2. The initial control polygon is associated with $\widetilde{X}_{16,1}$. Once again, after three levels of subdivision, the new control polygons are closer and closer to the graph of h_2. A few subdivision steps produce good results.

5. Conclusion

In this work, a rule has been proposed to construct C^2 cubic quasi-interpolants defined on a partition with a refinement that divides each interval into two sub-intervals instead of three. They have the same regularity that one constructed in [2–4] and the associated quasi-interpolation operators have the same order of convergence. The computational cost has been significantly reduced.

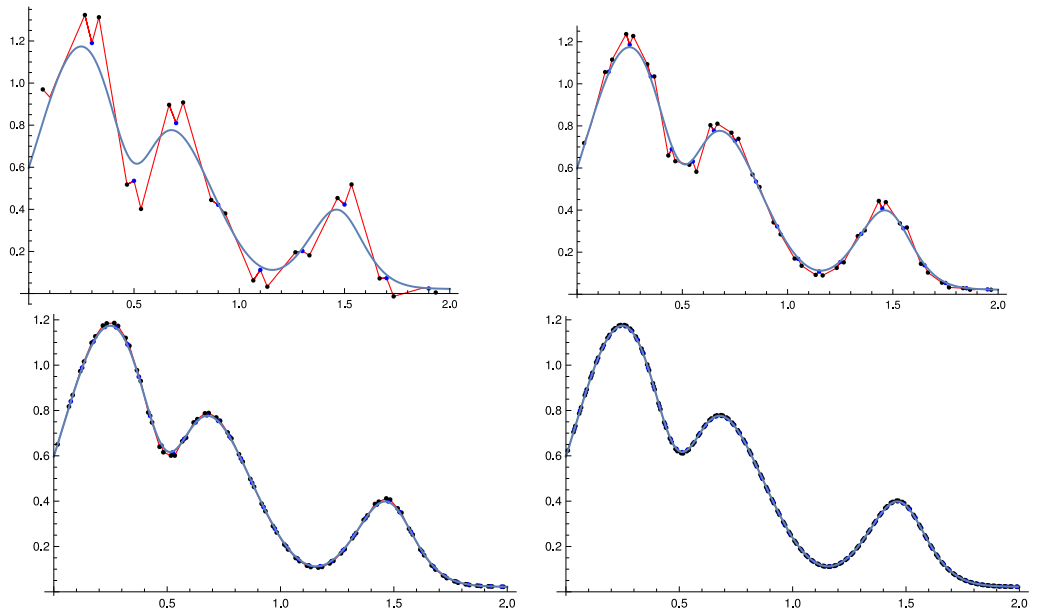

Fig. 8. From top to bottom and from left to right, plots of control polygons of h_1 given by levels $\widetilde{X}_{10,1}$, $\widetilde{X}_{10,2}$, $\widetilde{X}_{10,3}$ and $\widetilde{X}_{10,4}$ in red color and the plot of h_1 in blue color. The black points represent the control points $W_{i,j}$, while the blue ones stand for Z_k.

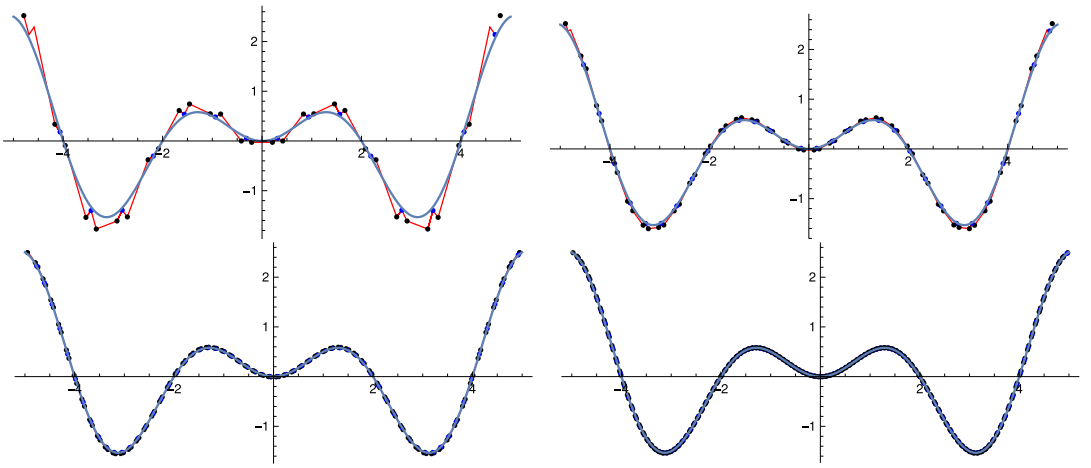

Fig. 9. From top to bottom and from left to right, plots of control polygons of h_2 given by levels $\widetilde{X}_{16,1}$, $\widetilde{X}_{16,2}$, $\widetilde{X}_{16,3}$ and $\widetilde{X}_{16,4}$ in red color and the curve of h_2 in blue color. The black points represent the control points $W_{i,j}$, while the blue ones stand for Z_k.

If the refined partition under consideration is further subdivided by adding a split point to each sub-interval, a C^2 cubic spline defined on the original partition and written in the corresponding basis of B-spline-like functions is expressed in terms of the basis functions associated with the new finer partition. The coefficients involved in both representations have been related by subdivision rules in both the uniform and non-uniform cases. These rules can be applied not only to splines with C^2 continuity but also to C^1 cubic splines C^2 continuous at the split points.

Several numerical tests have been included to show the good performance of both the procedure for constructing class two quasi-interpolants and the subdivision rules.

Data availability

No data was used for the research described in the article.

Acknowledgments

The authors wish to thank the anonymous referees for their very pertinent and useful comments which helped them to improve the original manuscript. The first author acknowledges partial financial support by the "María de Maeztu" Excellence Unit IMAG (University of Granada, Spain) grant CEX2020-001105-MICIN/AEI/10.13039/501100011033. The second author would like to thank the University of Granada for the financial support for the research stay during which this work was carried out.

Funding for open access charge: University of Granada / CBUA.

References

[1] W. Dahmen, T.N.T. Goodman, C.A. Micchelli, Compactly supported fundamental functions for spline interpolation, Numer. Math. 52 (1988) 639–664.
[2] D. Barrera, S. Eddargani, M.J. Ibáñez, A. Lamnii, A new approach to deal with C^2 cubic splines and its application to super-convergent quasi-interpolation, Math. Comput. Simulation 194 (2022) 401–415.
[3] A. Lamnii, M. Lamnii, F. Oumellal, Computation of Hermite interpolation in terms of B-spline basis using polar forms, Math. Comput. Simulation 134 (2017) 17–27.
[4] A. Rahouti, A. Serghini, A. Tijini, Construction of superconvergent quasi-interpolants using new normalized C^2 cubic B-splines, Math. Comput. Simulation 178 (2020) 603–624.
[5] L.L. Schumaker, On shape preserving quadratic spline interpolation, SIAM J. Numer. Anal. 20 (4) (1983) 854–864.
[6] H. Speleers, Multivariate normalized Powell–Sabin B-splines and quasi-interpolants, Comput. Aided Geom. Design 30 (2013) 2–19.
[7] D. Barrera, S. Eddargani, A. Lamnii, A novel B-spline basis for a family of many knot spline spaces and its application to quasi-interpolation, J. Comput. Appl. Math. 404 (2022) 113761.
[8] M. Powell, M. Sabin, Piecewise quadratic approximations on triangles, ACM Trans. Math. Softw., 3 (1977) 316–325.
[9] P. Dierckx, On calculating normalized Powell–Sabin B-splines, Comput. Aided Geom. Design 15 (1997) 61–78.
[10] M. Lamnii, H. Mraoui, A. Tijini, A. Zidna, A normalized basis for C^1 cubic super spline space on Powell–Sabin triangulations, Math. Comput. Simulation 99 (2015) 108–124.
[11] A. Lamnii, M. Lamnii, H. Mraoui, Cubic spline quasi-interpolants on Powell–Sabin partitions, BIT 54 (2014) 1099–1118.
[12] H. Speleers, A new B-spline representation for cubic splines over Powell–Sabin triangulations, Comput. Aided Geom. Design 37 (2015) 42–56.
[13] J. Grošelj, M. Krajnc, C^1 Cubic splines on Powell–Sabin triangulations, Appl. Math. Comput. 272 (2016) 114–126.
[14] J. Grošelj, H. Speleers, Construction and analysis of cubic Powell–Sabin B-splines, Comput. Aided Geom. Design 57 (2017) 1–22.
[15] D. Barrera, S. Eddargani, M.J. Ibáñez, A. Lamnii, A geometric characterization of Powell–Sabin triangulations allowing the construction of C^2 quartic splines, Comput. Math. Appl. 100 (2021) 30–40.
[16] J. Grošelj, M. Krajnc, Quartic splines on Powell–Sabin triangulations, Comput. Aided Geom. Design 49 (2016) 1–16.
[17] M. Lamnii, H. Mraoui, A. Tijini, Construction of quintic Powell–Sabin spline quasi-interpolants based on blossoming, J. Comput. Appl. Math. 250 (2013) 190–209.
[18] S. Eddargani, M.J. Ibáñez, A. Lamnii, M. Lamnii, D. Barrera, Quasi-interpolation in a space of C^2 sextic splines over Powell–Sabin triangulations, Mathematics 9 (2021) 2276.
[19] H. Speleers, Construction of normalized B-splines for a family of smooth spline spaces over Powell–Sabin triangulations, Constr. Approx. 37 (2013) 41–72.
[20] J. Grošelj, A normalized representation of super splines of arbitrary degree on Powell–Sabin triangles, BIT 56 (2016) 1257–1280.
[21] P. Alfeld, L.L. Schumaker, Smooth macro-elements based on Powell–Sabin triangle splits, Adv. Comput. Math. 16 (2002) 29–46.
[22] M.-J. Lai, L.L. Schumaker, Macro-elements and stable local bases for splines on Powell–Sabin triangulations, Math. Comp. 72 (2003) 335–354.
[23] A.J. Worsey, B. Piper, A trivariate Powell–Sabin interpolant, Comput. Aided Geom. Design 5 (1988) 177–186.
[24] T. Sorokina, A. Worsey, A multivariate Powell–Sabin interpolant, Adv. Comput. Math. 29 (2008) 71–89.
[25] M.L. Mazure, Blossoms and optimal bases, Adv. Comput. Math. 20 (2004) 177–203.
[26] J.M. Carnicer, J.M. Peña, Totally positive bases for shape preserving curve design and optimality of B-splines, Comput. Aided Geom. Design 11 (1994) 633–654.
[27] J.M. Carnicer, T.N.T. Goodman, J.M. Peña, Convexity preserving scattered data interpolation using Powell–Sabin elements, Comput. Aided Geom. Design 26 (2009) 779–796.
[28] J. Grošelj, H. Speleers, Super-smooth cubic Powell–Sabin splines on three-directional triangulations: B-spline representation and subdivision, J. Comput. Appl. Math. 386 (2021) 113245.
[29] L. Ramshaw, Blossoming: A Connect-the-Dots Approach to Splines, Tech. Rep. 19, Digital Systems Research Center, 1987.
[30] E. Vanraes, P. Dierckx, A. Bultheel, On the Choice of the PS-Triangles, Technical Report 353, Department of Computer Science, K.U. Leuven, Leuven, Belgium, 2003.
[31] C. de Boor, A Practical Guide to Splines, revised ed., Springer-Verlag, Berlin, New-York, 2001.
[32] A. Serghini, A. Tijini, Trivariate spline quasi-interpolants based on simplex splines and polar forms, Math. Comput. Simulation 118 (2015) 34–359.
[33] J. Grošelj, H. Speleers, Three recipes for quasi-interpolation with cubic Powell–Sabin splines, Comput. Aided Geom. Design 67 (2018) 47–70.
[34] R. Franke, Scattered data interpolation: Tests of some methods, Math. Comp. 38 (1982) 181–200.
[35] G.M. Nielson, A first order blending method for triangles based upon cubic interpolation, Internat. J. Numer. Methods Engrg. 15 (1978) 308–318.
[36] A. Boujraf, D. Sbibih, M. Tahrichi, A. Tijini, A super-convergent cubic spline quasi-interpolant and application, Afr. Mat. 26 (2015) 1531–1547.
[37] A. Boujraf, M. Tahrichi, A. Tijini, C^1 Super-convergent quasi-interpolation based on polar forms, Math. Comput. Simulation 118 (2015) 102–115.